



ELSEVIER

Contents lists available at ScienceDirect

Journal of Pharmaceutical Sciences

journal homepage: www.jpharmsci.org

Pharmacokinetics, Pharmacodynamics and Drug Transport and Metabolism

Model-Based Drug Development in Pulmonary Delivery: Pharmacokinetic Analysis of Novel Drug Candidates for Treatment of *Pseudomonas aeruginosa* Lung Infection



Tomás Sou^{1,2}, Irena Kukavica-Ibrulj³, Fadi Soukarieh⁴, Nigel Halliday⁴, Roger C. Levesque³, Paul Williams⁴, Michael Stocks⁵, Miguel Cámara⁴, Lena E. Friberg², Christel A.S. Bergström^{1,*}

¹ Department of Pharmacy, Uppsala University, Uppsala Biomedical Centre, Uppsala, Sweden

² Department of Pharmaceutical Biosciences, Uppsala University, Uppsala Biomedical Centre, Uppsala, Sweden

³ Institut de Biologie Intégrative et des Systèmes, Université Laval, Québec G1V 0A6, Canada

⁴ School of Life Sciences, Centre for Biomolecular Sciences, University of Nottingham, Nottingham NG7 2RD, UK

⁵ School of Pharmacy, Centre for Biomolecular Sciences, University of Nottingham, Nottingham NG7 2RD, UK

ARTICLE INFO

Article history:

Received 24 July 2018

Revised 16 September 2018

Accepted 17 September 2018

Available online 23 September 2018

Keywords:

pulmonary drug delivery

pharmacometrics

PK/PD modeling

preclinical pharmacokinetics

absorption

solubility

metabolic clearance

distribution

disposition

simulations

ABSTRACT

Antibiotic resistance is a major public health threat worldwide. In particular, about 80% of cystic fibrosis patients have chronic *Pseudomonas aeruginosa* (PA) lung infection resistant to many current antibiotics. We are therefore developing a novel class of antivirulence agents, quorum sensing inhibitors (QSIs), which inhibit biofilm formation and sensitize PA to antibiotic treatments. For respiratory conditions, targeted delivery to the lung could achieve higher local concentrations with reduced risk of adverse systemic events. In this study, we report the pharmacokinetics of 3 prototype QSIs after pulmonary delivery, and the simultaneous analysis of the drug concentration-time profiles from bronchoalveolar lavage, lung homogenate and plasma samples, using a pharmacometric modeling approach. In addition to facilitating the direct comparison and selection of drug candidates, the developed model was used for dosing simulation studies to predict *in vivo* exposure following different dosing scenarios. The results show that systemic clearance has limited impact on local drug exposure in the lung after pulmonary delivery. Therefore, we suggest that novel QSIs designed for pulmonary delivery as targeted treatments for respiratory conditions should ideally have a long residence time in the lung for local efficacy with rapid clearance after systemic absorption for reduced risk of systemic adverse events.

© 2019 The Authors. Published by Elsevier Inc. on behalf of the American Pharmacists Association®. This is an open access article under the CC BY-NC-ND license (<http://creativecommons.org/licenses/by-nc-nd/4.0/>).

Introduction

Antibiotic resistance is a growing challenge and a major public health threat worldwide. In particular, *Pseudomonas aeruginosa* (PA) exhibits high rates of resistance to many of the currently available antibiotic therapies.^{1,2} Previous reports have indicated that about 80% of patients with cystic fibrosis (CF) have chronic PA lung infections.^{3,4} New treatment options for these infections are therefore urgently required. Because the formation of a biofilm increases the tolerance of PA to antibacterial drugs,⁵⁻⁷ inhibition of the PA quorum-sensing (QS) signaling pathway, which regulates multiple

PA virulence factors as well as biofilm formation, has been suggested as a promising target.^{2,8-11} We are therefore developing a novel class of antivirulence agents, quorum sensing inhibitors (QSIs), with the aim of sensitizing PA biofilms to antibiotic treatment.

For respiratory conditions such as lung infections, targeted delivery of drugs directly to the site of action could provide unique benefits compared to systemic administration. Local delivery to the lung could achieve a higher local concentration at the target site with reduced systemic exposure and risk of adverse events.¹² However, despite the increasing interest in pulmonary delivery over the last few decades, compared to conventional oral dosage forms, the pharmacokinetics (PK) of drug molecules after pulmonary administration remains relatively poorly understood. Although plasma drug concentrations are commonly measured for estimating systemic drug exposure, the measurement of drug levels in the lung is

* Correspondence to: Christel A.S. Bergström (Telephone: +46-18-471 4118).

E-mail address: christel.bergstrom@farmaci.uu.se (C.A.S. Bergström).

not routinely carried out, typically because of the more difficult, labor-intensive sampling techniques and uncertainties in concentration determination methods. Consequently, there is no common standard in the sampling and measurement of lung PK.

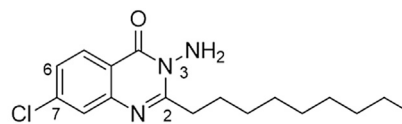
In the literature, antibiotic concentrations in the lung have been measured in samples collected from bronchoalveolar lavage (BAL), sputum, microdialysis, and lung tissue homogenates.¹³⁻¹⁸ However, these different sampling methods do not necessarily provide the same information. For instance, BAL and sputum samples are more likely to reflect extracellular drug concentrations, on the surface of the airways, whereas microdialysis samples are more likely to represent drug concentrations at a specific site of the lung parenchyma. In contrast, lung homogenates serve to provide a general estimation of total drug amounts in the lung and include both intracellular and extracellular drugs, with no indication of the specific site in the lung that was exposed to the drug delivery system. Although lung PK have been studied using one of these sampling approaches (i.e., BAL, sputum, lung homogenates, or microdialysis), to the best of our knowledge, few studies in the literature, if any, have collected and simultaneously analyzed drug concentrations in 3 sampling matrices (i.e., BAL, lung tissue homogenate, and plasma samples) from the same animals using a mathematical modeling approach to characterize the distribution of drugs between these physiological compartments.

In this study, we report the simultaneous modeling and analysis of drug concentrations in plasma and lung, with or without BAL sampling, of 3 prototype QSIs following pulmonary administration. SEN001 is a prototype QSI, which antagonizes the action of PqsR, a lysR-type regulator of the alkyl-quinolone (AQ)-dependent QS signaling system in PA, with promising *in vitro* activity.¹⁹ SEN019 and SEN032 are newly designed structural analogues of SEN001, which also antagonize PqsR and hence inhibit QS. These compounds were studied *in vivo* to investigate their therapeutic potential and suitability as drug candidates. The PK of the compound series following pulmonary administration was studied in rats, and the observed concentrations were simultaneously analyzed and modeled. The study demonstrated the use of pharmacometric modeling as a powerful tool to inform drug candidate selection in preclinical drug development of treatments for pulmonary delivery. During the analysis, a pharmacokinetic model was developed to describe all available observations from the compound series, and the estimated parameters provided quantitative insights into the distribution and clearance properties of the 3 QSI compounds. Furthermore, the model was able to quantify drug amounts in the lung before BAL collection, thus allowing direct comparison of local lung exposures between compounds, with or without BAL sampling. The developed model was then used to predict *in vivo* exposure following different dosing regimens to support the design of pharmacodynamics studies in disease models. The potential impact of systemic clearance on lung exposure to the drugs following pulmonary administration was also investigated.

Materials and Methods

Compounds

SEN001 (3-amino-7-chloro-2-nonylquinazolin-4(3H)-one),¹⁹ SEN019, and SEN032 are PqsR antagonists developed at the University of Nottingham. SEN001 and SEN019 were synthesized in house, whereas SEN032 was purchased from Enamine Ltd (Kiev, Ukraine). The structure of SEN001 is shown in Figure 1. SEN019 and SEN032 are structural analogues of SEN001, and the sites of modification from SEN001 are indicated with small numbers in Figure 1. The structures of SEN019 and SEN032 are not disclosed for



SEN001: 3-amino-7-chloro-2-nonylquinazolin-4(3H)-one

Figure 1. The structure of SEN001 with the numbers indicating the site of modifications.

intellectual property protection purposes because the compounds are patent-pending. Polyethylene 400 (PEG400) and polysorbate 80 (PS80) were purchased from Sigma-Aldrich (Stockholm, Sweden).

Compound Characterization

Measurements of melting point (T_m) of the compounds were performed by differential scanning calorimetry (DSC) using a DSC Q2000 (TA instrument), which was calibrated for temperature and enthalpy using indium. The instrument was equipped with a refrigerated cooling system. T_m was determined using an amount of 1-3 mg in nonhermetic sealed aluminum pans. The compounds were scanned at a heating rate of 10°C/min under a continuously purged dry nitrogen atmosphere (50 mL/min). Additional physicochemical properties were obtained *in silico* using ADMET Predictor Version 7.2 (Simulation Plus, Inc., Lancaster, CA). Two-dimensional SDF files of SEN001, SEN019 and SEN032, were introduced into the software, which evaluated the structures to calculate physicochemical and biopharmaceutical properties at pH 7.4. The physicochemical properties of the compound series are summarized in Table 1.

Solubility Determination

The equilibrium solubility of the crystalline compounds in various media was determined by adding excess of the solid compounds (2-3 mg) to 1 mL (or equivalent proportion) of either water or PP2% (a mixture of PS80 2% w/w and PEG400 2% w/w in water). Samples were incubated at 37°C for >24 h to allow dissolution. The supernatant was separated from the excess solid by centrifugation at 30,279 × g for at least 20 min (Heraeus Megafuge 8R Centrifuge with a MicroClick 24 × 2 mL rotor). The concentration of the compound in the supernatant was then determined by high-performance liquid chromatography with ultraviolet-detection (HPLC-UV).

Metabolic Stability

Briefly, metabolic stability of the compounds was determined in 0.5 mg/mL human liver microsomes at a compound concentration of 1 μM in 100 mM KPO4 buffer, pH 7.4, in a total incubation volume of 500 μL. The reaction was initiated by addition of 1 mM NADPH. At various incubation times (i.e., 0, 5, 10, 20, 40, and 60 min), a sample

Table 1
The Physicochemical Properties of SEN001, SEN019, and SEN032

Compound	MW	pKa	Log P	HBD	HBA	T_m (°C)	ΔH (J/g)
SEN001	321.85	3.29	5.11	1	3	79.7	136.2
SEN019	369.81	1.82	2.35	1	5	176.5	97.4
SEN032	319.81	2.89; 1.54	2.92	0	3	113.1	104.6

HBA, hydrogen bond acceptor; HBD, hydrogen bond donor; MW, molecular weight in g/mol; T_m , onset melting temperature; ΔH , melting enthalpy.

was withdrawn from the incubation, and the reaction in the sample was terminated by addition of cold acetonitrile. The amount of parent compound remaining was analyzed by liquid chromatography-tandem mass spectrometry (LC-MS/MS).

Pharmacokinetic Studies

The PK data of the compound series were collected from a number of studies in rats (male; Sprague-Dawley). The PK study of SEN001 was performed at Laval University in Quebec, Canada. The PK study of SEN019 and SEN032 was performed at Xenogesis (Nottingham, UK) and its animal research facility Saretius (Nottingham, UK). The study protocols were reviewed and approved by the respective animal ethics committee at Laval University and Saretius. The animals were carefully monitored throughout the studies for signs of toxicity.

The drugs were given via intratracheal (IT) administration to the lungs. Briefly, for SEN001, rats were lightly anesthetized with gaseous isoflurane and placed in a supine position on a restraining board angled at approximately 60° to 70° from the horizontal. The tongue of the rat was gently pulled outward using forceps, Q-tips, and the blade of a small animal otoscope (Hallowel EMC, Pittsfield, MA) was positioned in the distal part of the mouth to enable visualization of the vocal cords. An adapted 2 inches 16G intravenous catheter was then maneuvered past the vocal cords to the trachea-bronchus bifurcation. A 250 µL aliquot of the dosing solution was then administered into the lungs. Following IT administration, the rats were returned to metabolic cages where they rapidly recovered from the isoflurane anesthesia. The study of SEN019 and SEN032 was performed based on a similar protocol. The animals were administered SEN001, SEN019, and SEN032 at doses of 0.067 mg/kg, 0.12 mg/kg, and 0.28 mg/kg of body weight, respectively. The selection of doses was restricted by the aqueous solubility and availability of the compounds at the time. Blood, lung, and BAL samples were collected at predetermined time points, and the samples were analyzed by LC-MS. A summary of the PK study design is shown in Table 2.

Analytical Methods

For the solubility studies, the concentrations of the compounds in the samples were analyzed using an Agilent 1290 HPLC system (Agilent Technologies, Santa Clara, CA) equipped with a UV/Vis spectrometer DAD detector. The compounds were separated using an Agilent ZORBAX Eclipse XDB-C18, 3.5 µm, 4.6 × 100 mm. The column temperature was set to 50°C with a total run time of 4 (SEN019, SEN032) or 7 min (SEN001). The mobile phase was 80% v/v acetonitrile and 20% v/v water (SEN001, SEN032) or 70% v/v acetonitrile and 30% v/v water (SEN019), and the flow rate was 1 mL/min using an isocratic method. Absorbance of the compounds was monitored at 280 nm. The injection volume was 20 µL. Standard solutions were prepared by dissolving mixtures of the compounds in acetonitrile and analyzed with HPLC to prepare a calibration curve.

Table 2
Summary of the Design of the Pharmacokinetic Studies

Compound	N	Dose (mg/kg)	Time Points (h)	Sampling
SEN001	21	0.067	0.5, 2, 4, 8, 12, 24, 48	Plasma, lung and BAL
SEN019	18	0.12	0.167, 0.5, 1, 3, 6, 24	Plasma and lung
SEN032	18	0.28	0.167, 0.5, 1, 3, 6, 24	Plasma and lung

BAL, bronchoalveolar lavage; N, number of subjects.

For the metabolic stability studies, the amount of parent compound remaining in the microsome samples was analyzed by LC-MS/MS. Briefly, quantitative analysis was performed using a Waters XEVO TQ mass spectrometer (MS) in positive electrospray MRM mode coupled to an Acquity ultraperformance liquid chromatography (UPLC) system. The MS ion transitions were SEN001 322/180.1, SEN019 370/111, and SEN032 320/140. The analytes were separated using a Waters BEH C18 2 × 50 mm column over a 2-min run time. The mobile phases were double-distilled water with formic acid (0.1%) and acetonitrile with formic acid (0.1%).

For the PK study of SEN001, the amounts of the drug in the samples were quantified by LC-MS. Briefly, the analyte was extracted from plasma and lung homogenate samples by solvent extraction with ethyl acetate. BAL samples were extracted by solid phase extraction (Waters Oasis MCX extraction cartridges). The quantitative analysis was conducted using a Shimadzu series 10AD VP LC system in tandem with an Applied Biosystems Qtrap 4000 hybrid triple-quadrupole linear ion trap mass spectrometer. The chromatographic separation was achieved using a Phenomenex Gemini C18 column (3.0 µm, 50 × 3.0 mm). The mobile phases were 0.1% (v/v) formic acid in water and methanol. The MS ion transition used for analyte detection was precursor ion $[M + H]^+ = 322.2$ m/z, product ion $[M + H]^+ = 180.1$ m/z.

For the PK study of SEN019 and SEN032, the amounts of drugs in the samples were quantified by LC-MS. Briefly, the plasma and lung samples were treated with acetonitrile for protein precipitation. Quantitative analysis was then performed using a Thermo TSQ Quantiva mass spectrometer in positive electrospray MRM mode coupled to a Thermo Vanquish UPLC system. MS ion transitions were SEN019 370/181 and 370/237, and SEN032 320/71 and 320/140. The analytes were separated using a Phenomenex, Kinetex, biphenyl 2.6µm, 50 × 2.1 mm column over a 1.3-min run time. The mobile phases were Milli-Q water with formic acid (0.1%) and acetonitrile with formic acid (0.1%).

Pharmacokinetic Model Development

The data were first analyzed by noncompartmental analysis to obtain initial estimates. Model development was then performed in the nonlinear mixed-effects modeling software program NONMEM (version 7.3, ICON Development Solutions)²⁰ with Perl-speaks-NONMEM (PsN)²¹ using the Laplacian conditional estimation method with interaction algorithm. R (R Foundation for Statistical Computing, Vienna, Austria) with the Xpose package²² was used for model evaluation and graphical analysis. Initially, models were independently developed for SEN001, SEN019, and SEN032 to obtain key disposition parameters. The observed concentrations were then combined to simultaneously analyze the pharmacokinetic profiles of the 3 drugs after IT administration.

The general structural model developed in the analysis is illustrated in Figure 2. Briefly, it consists of 1 central lung compartment (L) where lung homogenate and BAL samples were taken, 1 deep lung compartment (LP) to describe the disposition of drugs in the lung before systemic absorption, 1 central plasma compartment (C) where plasma samples were taken, and 1 peripheral tissue compartment (P) to describe the disposition of the drugs after systemic absorption. During the analysis, 1-, 2-, 3-, and 4-compartment disposition models were evaluated; the transfers of drug between these compartments over time (t) are shown in Equations 1-4, where A is the amount of drug in each compartment, and V, CL, and Q are the volume of distribution, clearance, and intercompartmental clearance parameters of the corresponding compartments, respectively.

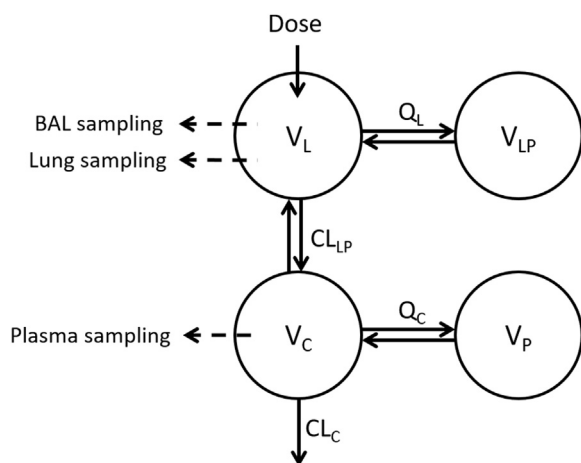


Figure 2. Schematic diagram of the general structural model developed for the analysis. Abbreviations: BAL, bronchoalveolar lavage; CL_C , central clearance; CL_{LP} , clearance from lung to plasma; Q_C , intercompartmental clearance between V_C and V_P ; Q_L , intercompartmental clearance between V_L and V_{LP} ; V_C , volume of the central plasma compartment; V_L , volume of the central lung compartment; V_P , volume of the peripheral tissue compartment; V_{LP} , volume of the deep lung compartment.

$$\frac{dA_L}{dt} = -\frac{CL_{LP}}{V_L} \cdot A_L + \frac{CL_{LP}}{V_C} \cdot A_C - \frac{Q_L}{V_L} \cdot A_L + \frac{Q_L}{V_{LP}} \cdot A_{LP} \quad (1)$$

$$\frac{dA_C}{dt} = \frac{CL_{LP}}{V_L} \cdot A_L - \frac{CL_{LP}}{V_C} \cdot A_C - \frac{CL_C}{V_C} \cdot A_C - \frac{Q_C}{V_C} \cdot A_C + \frac{Q_C}{V_P} \cdot A_P \quad (2)$$

$$\frac{dA_P}{dt} = \frac{Q_C}{V_C} \cdot A_C - \frac{Q_C}{V_P} \cdot A_P \quad (3)$$

$$\frac{dA_{LP}}{dt} = \frac{Q_L}{V_L} \cdot A_L - \frac{Q_L}{V_{LP}} \cdot A_{LP} \quad (4)$$

Where BAL samples were available, the addition of a separate compartment for BAL concentrations was also evaluated but this was not included in the final model. In the final model, the total amount of drug in the central lung compartment represents the sum of drug amounts in the BAL and lung samples. The concentrations of drug in the BAL samples (C_{BAL}) were quantified by estimating the fraction of drug collected in BAL (F_{BAL}) from the amount of drug in the central lung compartment (A_L) divided by the volume of fluid used to collect the BAL samples (V_{BAL}) as shown in Equation 5.

$$C_{BAL} = \frac{F_{BAL}}{V_{BAL}} \cdot A_L \quad (5)$$

During the analysis, the general structural model was developed and applied to analyze the observed concentrations of the 3 compounds and the fit of various models with and without the different compartments was evaluated. The volume of the central lung compartment was fixed to the typical size of lungs in a rat (2 g) to maintain model identifiability. The model parameters were scaled to the typical weight of the rats (0.3 kg) for comparability.

Because the majority of samples were terminal samples, interindividual variability (IIV) of the pharmacokinetic parameters was not estimated. The estimation of both IIV and residual unexplained variability with good precision requires more than 1 sample per subject. For residual unexplained variability, a mixed proportional and additive error model and a proportional error

Table 3
Solubility ($\mu\text{g/mL}$) of SEN001, SEN019, and SEN032 in Water and the PP2% Formulation (Mean \pm s.d., $n = 3$)

Medium	SEN001	SEN019	SEN032
Water	<LLOQ	20.2 ± 2.13	15.1 ± 0.34
PP2%	230.6 ± 3.08	182.7 ± 3.42	395.8 ± 3.13

LLOQ, lower limit of quantification (1 $\mu\text{g/mL}$); PP2%, PEG400 2% + PS80 2% w/w in water.

model were evaluated. Although most observation types were sufficiently well described by the proportional error model, the plasma concentrations of SEN019 and SEN032 were better described by the mixed error model. Data below the lower limit of quantification (LLOQ) were handled using the likelihood-based M3 method.²³

The likelihood ratio test was used to evaluate statistical significance for inclusion of additional parameters in nested models, where the objective function value (OFV) is assumed to be χ^2 distributed. A decrease in OFV of 3.84 between nested models with 1 parameter difference was considered to be a statistically significant difference at the 5% significance level. Model development was guided by the biological plausibility of the parameter estimates, the change in objective function value (ΔOFV), parameter precision, and evaluation of diagnostic plots. The final model was evaluated by performing a visual predictive check (VPC). For the VPC, 1000 data sets were simulated from the final parameter estimates using the original data set as a template. The predicted medians and their corresponding 95% confidence intervals were computed from the simulation data and overlaid with the observed values.

Drug Exposure Prediction Study

To compare the potential exposure of lung and plasma to various doses of SEN001, SEN019, and SEN032 following pulmonary administration, the parameter estimates of the final pharmacokinetic model were used to perform a dosing simulation study. The mrgsolve package (version 0.8.12.; Metrum Research Group) in the software R was used to carry out the simulation. The mean dose in the PK studies, 0.15 mg/kg, was used to compute the predicted concentration-time profiles for a dose-normalized exposure comparison, and drug concentrations were predicted when the compounds were given every 24, 12, and 8 h.

To investigate the potential impact of systemic clearance on lung and systemic exposures to the drugs, predictions were generated from a virtual population composed of 1000 simulated data sets with variability in central clearance (CL_C). Since physiological parameters are typically log-normally distributed, IIV was applied to CL_C using an exponential model, as shown in Equation 6, where CL_i is the individual clearance, CL is the typical clearance of the population, and η is normally distributed with a coefficient of variance (CV) of 30% around mean 0.

$$CL_i = CL \cdot e^\eta \quad (6)$$

Table 4
Metabolic Stability of SEN001, SEN019, and SEN032 in Human Liver Microsomes

Compound	Half-Life (min)	CL_{int} (mL/min)	CL_H (mL/min)	E_H
SEN001	54.4	1491.7	747.9	0.50
SEN019	22.0	3692.1	1066.7	0.71
SEN032	3.3	24,886.7	1414.7	0.94

CL_{int} , intrinsic clearance; CL_H , hepatic clearance; E_H , hepatic extraction ratio.

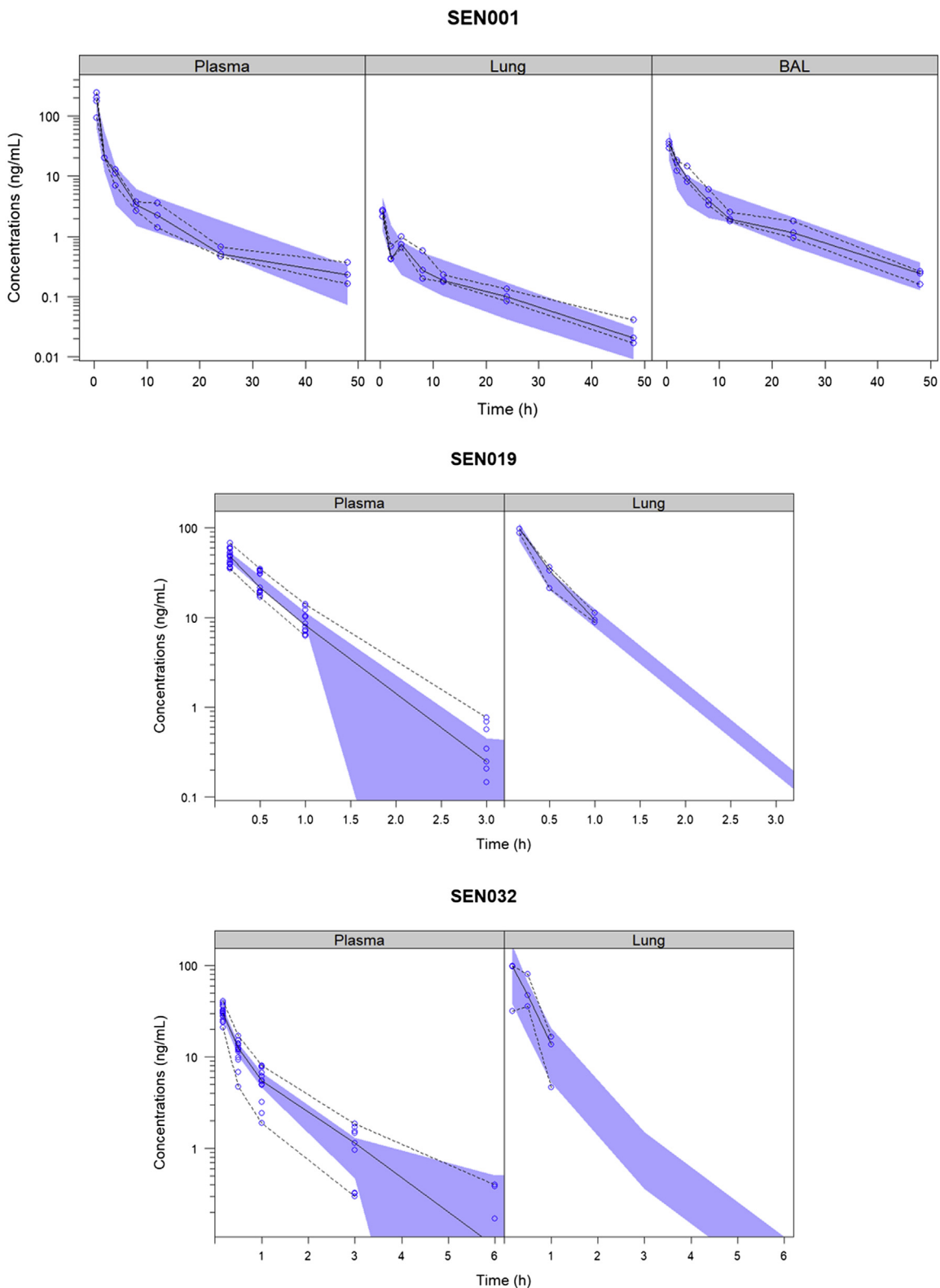


Figure 3. Visual predictive check of the final model showing the observed concentrations of SEN001, SEN019, and SEN032 in plasma, lung, and bronchoalveolar lavage (BAL) with the observed medians, 2.5th and 97.5th percentiles following intratracheal administration and the corresponding 95% confidence intervals of the predicted medians (shaded).

Table 5
Parameter Estimates and Relative Standard Errors of the Final Model

Parameter ^a	Unit ^b	Description	SEN001	% RSE	SEN019	% RSE	SEN032	% RSE
CL _{LP}	L/h	Clearance—lung to plasma	0.0175	7	0.0724	1	0.150	10
V _L	L	Volume of distribution—central lung	0.002	—	0.002	—	0.002	—
CL _C	L/h	Clearance—central	0.0745	10	1.11	5	3.74	6
V _C	L	Volume of distribution—central	0.0855	31	0.583	5	1.51	12
Q _C	L/h	Intercompartmental clearance—central	—	—	—	—	2.35	25
V _P	L	Volume of distribution—peripheral	—	—	—	—	1.36	35
Q _L	L/h	Intercompartmental clearance—lung	0.00596	37	—	—	0.0107	17
V _{LP}	L	Volume of distribution—deep lung	0.0582	19	—	—	0.00360	15
F _{BAL}	%	Fraction in BAL	0.980	0.3	—	—	—	—
PROP _{PL}	%	Proportional error—plasma	45.9	12	24.8	7	25.3	15
ADD _{PL}	µg/L	Additive error—plasma	—	—	0.284	22	0.505	42
PROP _{LG}	%	Proportional error—lung	43.5	13	18.1	25	46.1	30
PROP _{BAL}	%	Proportional error—BAL	38.0	22	—	—	—	—

BAL, bronchoalveolar lavage; RSE, relative standard error.

^a CL and V are apparent pharmacokinetic parameters following intratracheal administration and additive errors are expressed as variance.

^b Parameters are scaled to 0.3 kg (typical weight of rats).

Results

Formulation Development

The solubility of SEN001, SEN019, and SEN032 in water and the PP2% formulation is shown in Table 3. The compounds had poor aqueous solubility and the measured equilibrium solubility values ranged from <1 to 20.2 µg/mL. The PP2% formulation improved the solubility of the drugs significantly and increased the amount of solubilized drugs to >180 µg/mL. In addition, PP2% did not cause any detectable acute toxicity to the lungs of the animals, as supported by histological examination of the terminal lung samples. PP2% was therefore used to deliver solubilized drugs for IT administration in the PK studies.

Metabolic Stability

The metabolic stability results for SEN001, SEN019, and SEN032 in human liver microsomes are shown in Table 4. Overall, the results suggested that the metabolic stability of SEN001 was superior to that of SEN019 and SEN032. SEN019 and SEN032 were more likely to be rapidly cleared *in vivo* after systemic absorption as a result of extensive metabolism, as demonstrated by their high hepatic extraction ratios of 0.71 and 0.94, respectively.

Plasma Pharmacokinetics Following Pulmonary Administration

Following pulmonary administration, SEN001, SEN019, and SEN032 were rapidly absorbed from lung to the plasma, as demonstrated by the rapid appearance of the drugs in plasma shortly after administration and the lack of a discernible absorption phase in the plasma concentration-time profiles (Fig. 3). After absorption from the lung, the plasma concentrations of SEN001 declined steadily over the sampling period. In contrast, the concentrations of SEN019 and SEN032 in plasma declined more rapidly and were below the LLOQ after 3 h and 6 h, respectively.

Lung Pharmacokinetics Following Pulmonary Administration

The concentrations of SEN001 in lung and BAL declined more rapidly during the initial absorption and distribution into plasma and deep lung tissue. After reaching distribution equilibrium at 2 h, the decline in lung and BAL concentrations reflected the decline in plasma concentrations during the elimination phase. The lung and

BAL concentrations were closely correlated throughout the sampling period. In contrast, the concentrations of SEN019 and SEN032 in the lung fell below the LLOQ after 1 h.

Pharmacokinetic Modeling

The observed concentrations of the 3 drugs were all well described by the model with good predictive performance as demonstrated in the VPC (Fig. 3). Although the deep lung compartment (V_{LP}) was needed to describe the observed concentrations for SEN001, the addition of a peripheral compartment (V_P) did not result in statistically significant improvement in the model fit ($\Delta\text{OFV} = -0.643$). Neither the peripheral compartment (V_P) nor the deep lung compartment (V_{LP}) was needed to describe the observed concentrations for SEN019. In contrast, the four-compartment disposition model best described the observed concentrations for SEN032. The full model resulted in a statistically significant improved model fit compared to the reduced models without either the peripheral compartment (V_P) or the deep lung compartment (V_{LP}) ($\Delta\text{OFV} = -9.054$ and -10.47 , respectively).

The final model described the drug concentration-time profiles of the plasma, lung, and BAL samples, allowing direct comparison of pharmacokinetic properties between the compounds with and without BAL sampling. During model development, an additional compartment was evaluated for the BAL samples, but this did not reflect the drug disposition kinetics. In contrast, the observed concentrations in the lung and BAL samples were best described when the amounts of drug in the 2 samples were combined in the central lung compartment and F_{BAL} was estimated. The parameter estimates of the final model and the relative standard errors are summarized in Table 5.

Predicted Lung and Plasma Exposure Following Different Dosing Regimens

The concentrations of SEN001 in the lung before BAL collection were calculated from the model, and a dose-normalized exposure comparison was performed using the predicted concentrations in lung and plasma following IT administration of the 3 compounds every 24, 12, and 8 h (Figs. 4 and 5). The predicted profiles indicated that the concentrations of SEN001 in lung before BAL collection were much higher than those of the other 2 compounds. In contrast, SEN019 and SEN032 were rapidly cleared from both lung and

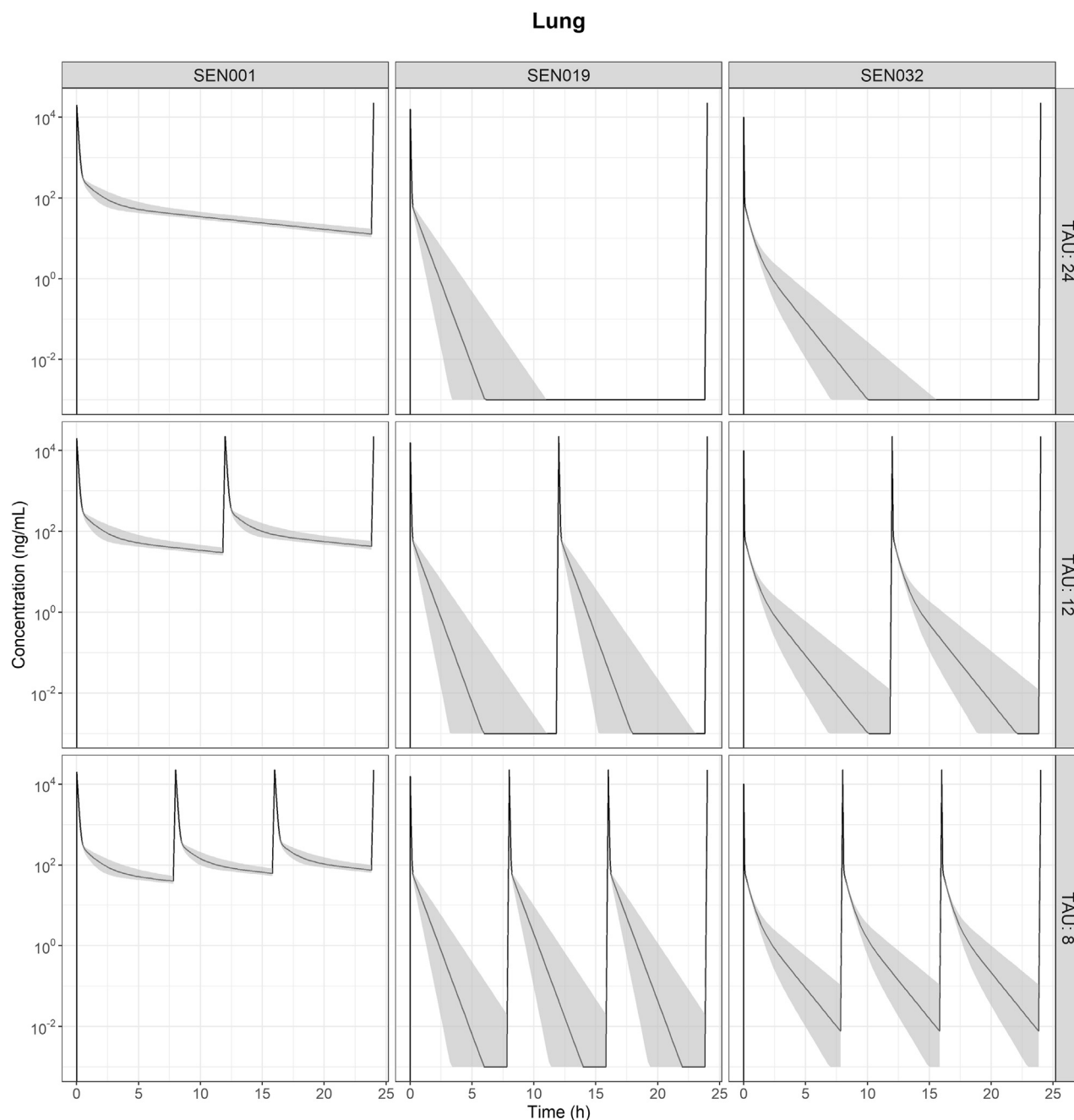


Figure 4. The predicted drug concentration versus time profiles in lung showing the predicted median concentrations (line) and the corresponding 95% prediction intervals (shaded) computed from the 1000 data sets in the simulated population with variability (CV of 30%) in central clearance (CL_C) following intratracheal administration of SEN001, SEN019, and SEN032 at 0.15 mg/kg every 24, 12, and 8 h (TAU).

plasma with minimal exposure following the different dosing regimens. The predicted lung and plasma exposure to SEN019 and SEN032 remained much lower than that to SEN001 administered every 24 h, even after more frequent dosing (up to every 12 and 8 h) and with variability in systemic clearance being taken into account, as demonstrated by the substantially lower area under the concentration-time curve (AUC) (Fig. 6). In addition, the impact of systemic clearance on lung concentrations appeared to be limited. Although the variability in plasma AUC resulting from the variability in central clearance ranged from 28.6% to 31.6%, the variability in lung AUC resulting from the same variability in central clearance ranged from only 1.2% to 5.3%.

Discussion

This study set out to investigate the pharmacokinetic properties of 3 prototype QSIs, SEN001, SEN019, and SEN032, being developed for the treatment of chronic PA lung infections, by collectively analyzing the observed concentrations from the PK studies. Because high local concentrations are desirable for treating lung infections, we focused on comparing drug concentrations in the lung following pulmonary administration. To remove the effect of dissolution, a solution was selected as the formulation of choice. Given the poor aqueous solubility of SEN001, chemical modifications were made to reduce the lipophilicity of this compound. The resulting SEN019 and SEN032 had, despite the lower logP, only

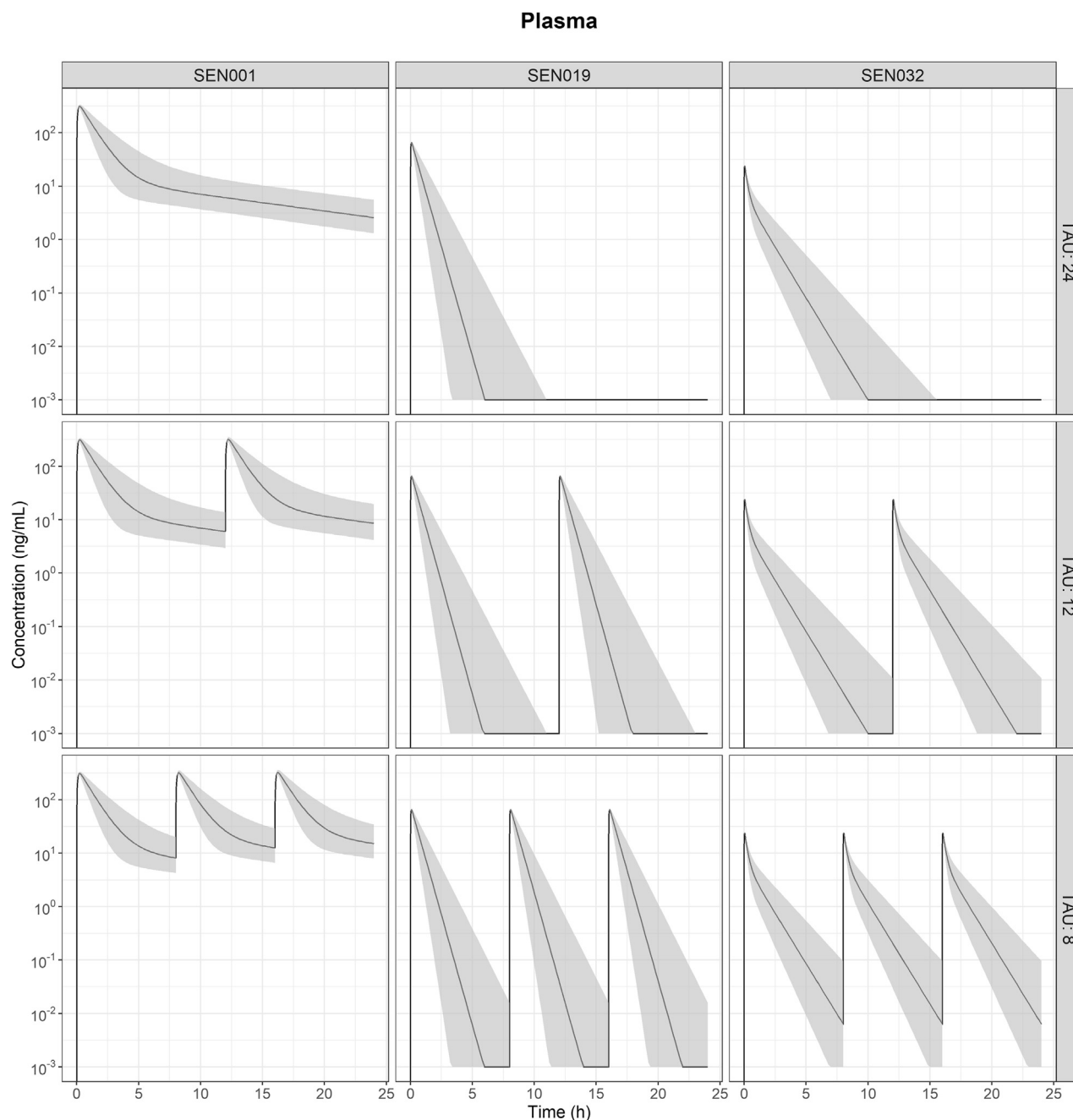


Figure 5. The predicted drug concentration versus time profiles in plasma showing the predicted median concentrations (line) and the corresponding 95% prediction intervals (shaded) computed from the 1000 data sets in the simulated population with variability (CV of 30%) in central clearance (CL_c) following intratracheal administration of SEN001, SEN019, and SEN032 at 0.15 mg/kg every 24, 12, and 8 h (TAU).

moderately improved aqueous solubility. Hence, we developed a pulmonary formulation that effectively solubilized the compounds, using excipients that have previously been used in the lung.²⁴⁻²⁶ Being the most soluble compound in water in the series, SEN019 appeared to interact least with the solubilizing agents and was the least soluble compound of the 3 in the formulation. Nevertheless, this PP2% formulation significantly enhanced the solubility of the compounds, allowing administration of the drugs in solution via the pulmonary route. Consequently, drug dissolution and particle clearance from the lung (e.g., mucociliary clearance) were not considered in the model.

The pharmacokinetic properties of the compounds following IT administration were then investigated in rats. In the first PK study, SEN001 was administered and drug concentrations in plasma, lung, and BAL were evaluated. It was apparent that the drug was rapidly absorbed from the lung, as demonstrated by its early appearance in plasma. The large surface area and very thin alveolar epithelial lining of the lung have long been suggested to allow rapid systemic absorption.²⁷⁻²⁹ In fact, rapid systemic absorption from the lung, with peak plasma concentrations reached in 5 min, has also been observed after IT administration of other drugs.^{15,30-32} The plasma concentration-time profile of SEN001 was consistent with the rapid

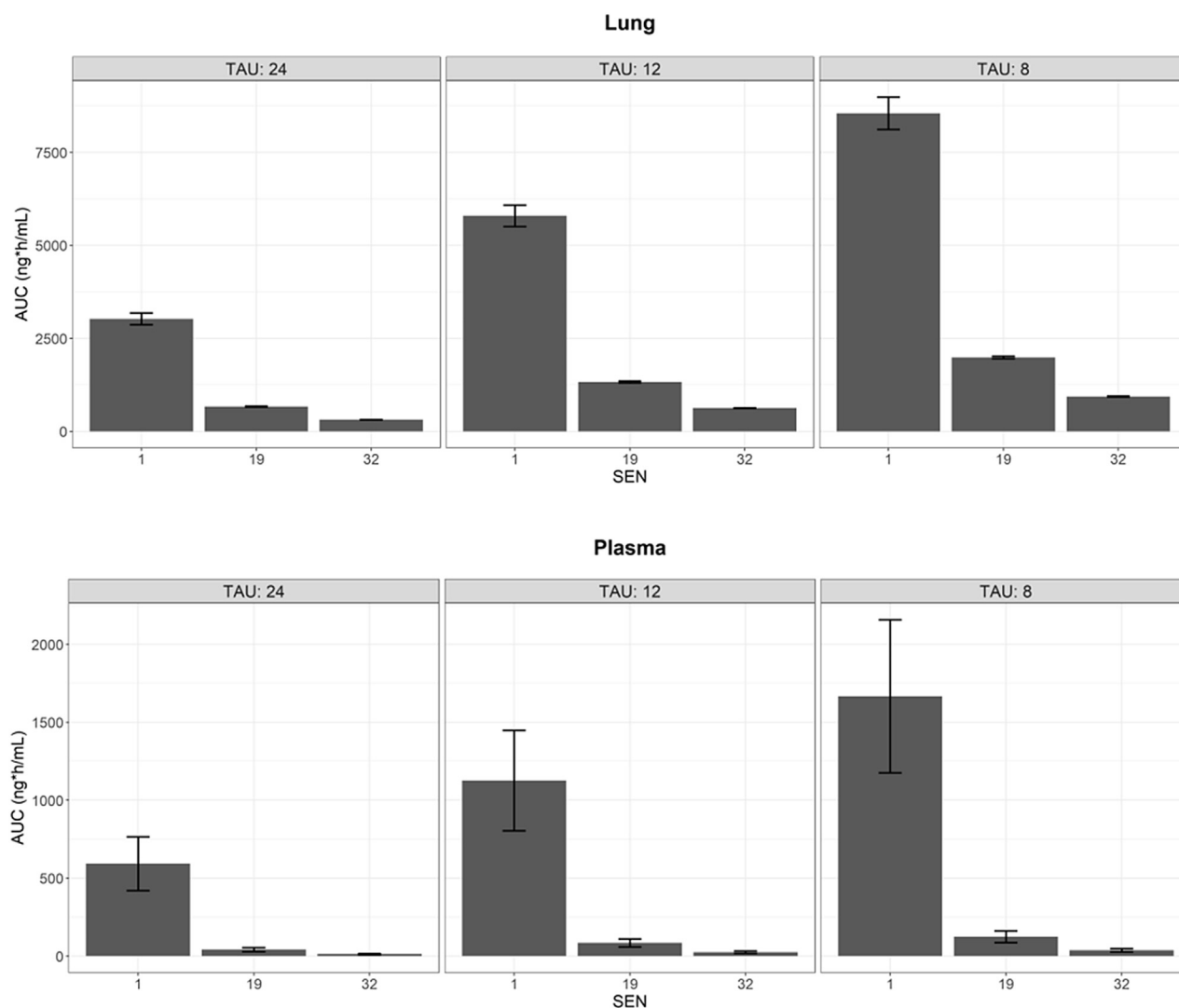


Figure 6. The area under the concentration-time curve (AUC) over 24 h computed from the predicted lung (top) and plasma (bottom) concentration-time profiles of the 1000 data sets in the simulated population [means \pm s.d.] following intratracheal administration of SEN001, SEN019, and SEN032 at 0.15 mg/kg every 24, 12, and 8 h (TAU).

absorption previously reported following effective pulmonary delivery.

The decline of SEN001 concentrations in the lung homogenate and BAL samples mirrored its decline in the plasma samples after distribution equilibrium at 2 h. The concentrations of SEN001 in the lung and BAL samples were closely correlated throughout the whole sampling period, suggesting colocation of the drug sampled from the BAL and lung homogenate, with no kinetically discernible distribution phase. The pharmacokinetic model strengthened this hypothesis, since the addition of a separate distribution compartment for drug amount in BAL did not improve the characterization of the data. In contrast, the observed concentrations were well described when the amounts of the drug in lung and BAL were considered in the same compartment, and the distribution of drugs into plasma and deep lung was dependent on the total amount of drug in the central lung compartment. The fraction of the drug that remained in the airway was then collected in BAL from the central lung. Consequently, the model allowed quantification of the drug amount in the lung before BAL collection, and hence the direct comparison of lung exposures to other compounds without BAL sampling.

Lung PK are typically investigated by collecting either lung homogenates from small animals for total lung exposures, fluids from the airways (e.g., BAL or sputum) as an indication of the amount of drug in the epithelial lining fluid, or microdialysis for drug concentrations at a specific site in the lung.^{13,15,16,31-34} While total lung concentrations provide an estimate of overall lung exposure, they might not always represent the most relevant therapeutic exposure, since the amounts of intracellular and extracellular drugs are indistinguishable from each other. Depending on the location of the drug target, either intracellular or extracellular concentrations are likely to be more applicable. Although BAL sampling is subject to potential contamination with intracellular drugs released from cells that rupture before or during the procedure, it can serve to provide an initial indication of the amount of extracellular drug concentration.

Although drug transfer between BAL and plasma has been previously described using a modeling approach for the study of other antibiotics and antituberculosis drugs,^{15,35-37} few studies in the literature have simultaneously modeled and analyzed observed drug concentration-time profiles of plasma, BAL, and lung homogenate samples collected from the same animals using a

quantitative approach. The results in the present study demonstrate the close relationship between SEN001 concentrations in BAL and the lung. The estimated fraction of SEN001 in BAL (F_{BAL}) suggested that most (>98%) of the SEN001 in the lung was likely residing on the epithelial lining of the airways, instead of being sequestered intracellularly, before systemic absorption.

SEN019 and SEN032 were developed as structural analogues of SEN001. Given the lack of a discernible distribution phase between BAL and lung parenchyma for SEN001, BAL samples were not collected for SEN019 and SEN032. The concentrations of these 2 compounds appeared to decline more rapidly than those of SEN001. In addition, the LLOQs for SEN019 and SEN032 in the lung samples were different from that for SEN001, making direct comparisons of drug concentration-time profiles difficult. A pharmacokinetic model was therefore developed, using all of the observed concentrations available, for the characterization and comparison of the compound series.

The model described all of the concentration-time profiles of the compound series following pulmonary administration, allowing direct comparison of pharmacokinetic parameters between compounds. Although all 3 compounds appeared in plasma shortly after IT administration, SEN001 had the most favorable pharmacokinetic properties for targeted treatment in the lung, with the longest residence time in the lung after pulmonary administration, as demonstrated by the slowest clearance from lung to plasma (CL_{LP}) and the additional deep lung compartment (V_{LP}) in the model. In contrast, the estimated CL_{LP} of SEN032 was 107% and 757% higher than that of SEN019 and SEN001, respectively. It seems likely that SEN001, with the highest logP, distributed most widely into deep lung tissue, resulting in the slowest clearance to plasma and the longest residence time in the lung. Conversely, SEN019, with the lowest logP, did not distribute extensively after delivery, as illustrated by the lack of deep lung and peripheral compartment in the model, resulting in rapid elimination of the drug. In addition, SEN032 was also most rapidly cleared following systemic absorption, as shown by the highest central clearance (CL_{C}). These results mirrored our findings on the metabolic stability of the compounds.

At first glance, the peak lung concentrations of SEN001 appeared much lower than those of SEN019 and SEN032. However, the SEN019 and SEN032 lung samples were analyzed directly, without BAL sampling. To compare concentrations in lung and plasma under standardized conditions, the model was used to perform a dose-normalized exposure analysis, by comparing the predicted drug concentrations in the lung and plasma following pulmonary administration of the same dose every 24, 12, and 8 h. Because the model allowed the estimation of lung concentrations before BAL sampling, direct comparison of lung concentrations between the compounds was possible. The results showed that SEN001 would reach much higher local concentrations in the lung after pulmonary administration compared to SEN019 and SEN032 (Figs. 4 and 5). Even after multiple dosing up to every 8 h, it was unlikely that the lung and plasma exposures to SEN019 and SEN032 would be similar to SEN001 given every 24 h, as demonstrated by the much lower predicted exposures (AUC) from the simulated profiles (Fig. 6).

Although it is intuitive that physiological processes in the lung (e.g., mucociliary clearance and absorption from the lung) could impact on drugs available locally to treat lung infections, it is difficult to directly evaluate the influence of systemic clearance on local drug exposure in the lung following pulmonary delivery. Hence, drug exposures were predicted using the model with variability in the central clearance (CL_{C}) parameter to investigate the specific impact of systemic clearance on lung concentrations of the compounds. The results showed that systemic clearance was unlikely to be the major factor impacting local drug exposure

in the lung. It is therefore unlikely that the low SEN019 and SEN032 exposures could be improved by reducing systemic clearance. In contrast, lower systemic clearance could lead to a much more influential increase in systemic drug exposure and therefore an increased risk of systemic adverse effects. We therefore suggest that novel QSIs designed for direct delivery to the lung for targeted treatment of respiratory conditions should ideally have long residence times in the lung for maximum local exposure and efficacy with rapid clearance after systemic absorption to reduce the risk of unwanted systemic adverse effects. This design strategy is consistent with the approach advocated for other local inhaled therapies such as inhaled corticosteroids,^{38–40} and the present study provides further quantitative insights into the underlying drug dispositions resulting from such a delivery strategy using a mathematical modeling approach. Similar design principles should also be considered for local antimicrobial therapies.

Although it is certainly of relevance to understand the PK of newly synthesized compounds in healthy animals during the candidate selection process, it should be noted that the local airway conditions in CF lungs with chronic PA infection are quite different compared to the ones in healthy animals. The presence of thick and viscous mucus could potentially hinder the clearance of drugs from the airways and alter their local PK profiles. In addition, the barriers that biofilms present to drug penetration to the microorganisms could have implications on the local residence time required for efficacy. Nonetheless, the results of the present study provide invaluable insights into the potential exposure of these compounds following pulmonary delivery. To further explore their therapeutic potential, studies to investigate the *in vivo* efficacy of these compounds in a relevant disease model would be beneficial.

Conclusions

This study has demonstrated a number of applications where pharmacometric modeling can be used as a powerful tool to inform drug development for pulmonary delivery in a preclinical setting, including the direct comparison of the pharmacokinetic properties of compounds to facilitate drug candidate selection, the prediction of *in vivo* exposure following different dosing regimens, and the identification of ideal pharmacokinetic properties to guide the future development of the treatment. This is one of the few studies reported in the literature in which drug concentration-time profiles of BAL, lung homogenate, and plasma samples were modeled and analyzed simultaneously to study lung PK. In addition, based on the predicted drug exposures, we suggest that novel QSIs designed for pulmonary delivery as targeted treatments for respiratory conditions should ideally have long residence times in the lung for local efficacy, with rapid clearance after systemic absorption to reduce the risk of unwanted systemic adverse effects. The developed model can also be connected to an infection model to study drug exposure-response relationships to improve the understanding of the pharmacokinetic-pharmacodynamic relationships of QSIs. Studies to develop QSIs as a novel treatment option for chronic PA lung infections are currently being undertaken.

Acknowledgments

This work was supported by the Joint Programming Initiative on Antimicrobial Resistance (JPIAMR). In UK, this work was also supported by the Medical Research Council [grant number MR/N501852/1] and by the Biotechnology and Biological Sciences Research Council [grant number BB/R012415/1]. The authors thank Richard Svensson and Uppsala University Drug Optimisation and Pharmaceutical Profiling Platform (UDOPP) for their assistance in

the measurements of metabolic stability, and XenoGesis (Nottingham, UK) for their assistance in the *in vivo* studies. We are grateful to Simulations Plus (Lancaster, CA) for providing the Drug Delivery Group at the Department of Pharmacy, Uppsala University with a reference site license for the software ADMET Predictor™.

References

- Chatterjee M, Anju CP, Biswas L, Anil Kumar V, Gopi Mohan C, Biswas R. Antibiotic resistance in *Pseudomonas aeruginosa* and alternative therapeutic options. *Int J Med Microbiol*. 2016;306(1):48-58.
- Ciofu O, Tolker-Nielsen T, Jensen PØ, Wang H, Høiby N. Antimicrobial resistance, respiratory tract infections and role of biofilms in lung infections in cystic fibrosis patients. *Adv Drug Deliv Rev*. 2015;85:7-23.
- Crull MR, Ramos KJ, Caldwell E, Mayer-Hamblett N, Aitken ML, Goss CH. Change in *Pseudomonas aeruginosa* prevalence in cystic fibrosis adults over time. *BMC Pulm Med*. 2016;16(1):176.
- Høiby N. Recent advances in the treatment of *Pseudomonas aeruginosa* infections in cystic fibrosis. *BMC Med*. 2011;9(1):1-7.
- de la Fuente-Núñez C, Reffuveille F, Fernández L, Hancock REW. Bacterial biofilm development as a multicellular adaptation: antibiotic resistance and new therapeutic strategies. *Curr Opin Microbiol*. 2013;16(5):580-589.
- Hengzhuang W, Wu H, Ciofu O, Song Z, Hoiby N. Pharmacokinetics/pharmacodynamics of colistin and imipenem on mucoid and nonmucoid *Pseudomonas aeruginosa* biofilms. *Antimicrob Agents Chemother*. 2011;55(9):4469-4474.
- Jolivet-Gougeon A, Bonnaure-Mallet M. Biofilms as a mechanism of bacterial resistance. *Drug Discov Today Technol*. 2014;11(Supplement C):49-56.
- Brackman G, Cos P, Maes L, Nelis HJ, Coenye T. Quorum sensing inhibitors increase the susceptibility of bacterial biofilms to antibiotics *in vitro* and *in vivo*. *Antimicrob Agents Chemother*. 2011;55(6):2655-2661.
- Gui N, Fan J, Cen K. Effect of particle-particle collision in decaying homogeneous and isotropic turbulence. *Phys Rev E Stat Nonlin Soft Matter Phys*. 2008;78(4):046307.
- Brackman G, Coenye T. Quorum sensing inhibitors as anti-biofilm agents. *Curr Pharm Des*. 2015;21(1):5-11.
- Hurley MN, Camara M, Smyth AR. Novel approaches to the treatment of *Pseudomonas aeruginosa* infections in cystic fibrosis. *Eur Respir J*. 2012;40(4):1014-1023.
- Falagas ME, Michalopoulos A, Metaxas EI. Pulmonary drug delivery systems for antimicrobial agents: facts and myths. *Int J Antimicrob Agents*. 2010;35(2):101-106.
- Torres BGS, Helfer VE, Bernardes PM, et al. Population pharmacokinetic modeling as a tool to characterize the decrease in ciprofloxacin free interstitial levels caused by *Pseudomonas aeruginosa* biofilm lung infection in wistar rats. *Antimicrob Agents Chemother*. 2017;61(7).
- Heng S-C, Snell GI, Levvey B, et al. Relationship between trough plasma and epithelial lining fluid concentrations of voriconazole in lung transplant recipients. *Antimicrob Agents Chemother*. 2013;57(9):4581-4583.
- Yapa SWS, Li J, Porter CJH, Nation RL, Patel K, McIntosh MP. Population pharmacokinetics of colistin methanesulfonate in rats: achieving sustained lung concentrations of colistin for targeting respiratory infections. *Antimicrob Agents Chemother*. 2013;57(10):5087-5095.
- Yapa SWS, Li J, Patel K, et al. Pulmonary and systemic pharmacokinetics of inhaled and intravenous colistin methanesulfonate in cystic fibrosis patients: targeting advantage of inhalational administration. *Antimicrob Agents Chemother*. 2014;58(5):2570-2579.
- Hendrickx R, Bergström EL, Janzén DLI, et al. Translational model to predict pulmonary pharmacokinetics and efficacy in man for inhaled bronchodilators. *CPT Pharmacometrics Syst Pharmacol*. 2018;7(3):147-157.
- Marchand S, Chauzy A, Dahyot-Fizeliez C, Couet W. Microdialysis as a way to measure antibiotics concentration in tissues. *Pharmacol Res*. 2016;111:201-207.
- llangovan A, Fletcher M, Rampioni G, et al. Structural basis for native agonist and synthetic inhibitor recognition by the *Pseudomonas aeruginosa* quorum sensing regulator PqsR (MvfR). *PLoS Pathog*. 2013;9(7):e1003508.
- Beal S, Sheiner LB, Boeckmann A, Bauer RJ. *NONMEM User's Guides (1989-2009)*. Ellicott City, MD: Icon Development Solutions ed.; 2009.
- Lindbom L, Ribbing J, Jonsson EN. Perl-speaks-NONMEM (PsN)—a Perl module for NONMEM related programming. *Comput Methods Programs Biomed*. 2004;75(2):85-94.
- Jonsson EN, Karlsson MO. Xpose—an S-PLUS based population pharmacokinetic/pharmacodynamic model building aid for NONMEM. *Comput Methods Programs Biomed*. 1998;58(1):51-64.
- Beal SL. Ways to fit a PK model with some data below the quantification limit. *J Pharmacokinet Pharmacodyn*. 2001;28(5):481-504.
- Pilcer G, Amighi K. Formulation strategy and use of excipients in pulmonary drug delivery. *Int J Pharm*. 2010;392(1-2):1-19.
- Traini D, Young PM, Rogueda P, Price R. Investigation into the influence of polymeric stabilizing excipients on inter-particulate forces in pressurized metered dose inhalers. *Int J Pharm*. 2006;320(1-2):58-63.
- Respaud R, Marchand D, Parent C, et al. Effect of formulation on the stability and aerosol performance of a nebulized antibody. *MAbs*. 2014;6(5):1347-1355.
- Labiris NR, Dolovich MB. Pulmonary drug delivery. Part I: physiological factors affecting therapeutic effectiveness of aerosolized medications. *Br J Clin Pharmacol*. 2003;56(6):588-599.
- Patton JS, Fishburn CS, Weers JG. The lungs as a portal of entry for systemic drug delivery. *Proc Am Thorac Soc*. 2004;1(4):338-344.
- Uchenna Agu R, Ikechukwu Ugwoke M, Armand M, Kinget R, Verbeke N. The lung as a route for systemic delivery of therapeutic proteins and peptides. *Respir Res*. 2001;2(4):198-209.
- Lin Y-W, Zhou QT, Cheah S-E, et al. Pharmacokinetics/pharmacodynamics of pulmonary delivery of colistin against *Pseudomonas aeruginosa* in a mouse lung infection model. *Antimicrob Agents Chemother*. 2017;61(3).
- Stass H, Delesen H, Nagelschmitz J, Staab D. Safety and pharmacokinetics of ciprofloxacin dry powder for inhalation in cystic fibrosis: a phase I, randomized, single-dose, dose-escalation study. *J Aerosol Med Pulm Drug Deliv*. 2015;28(2):106-115.
- Stass H, Weimann B, Nagelschmitz J, Rolinck-Werninghaus C, Staab D. Tolerability and pharmacokinetic properties of ciprofloxacin dry powder for inhalation in patients with cystic fibrosis: a phase I, randomized, dose-escalation study. *Clin Ther*. 2013;35(10):1571-1581.
- Tenero D, Bowers G, Rodvold KA, et al. Intrapulmonary pharmacokinetics of GSK2251052 in healthy volunteers. *Antimicrob Agents Chemother*. 2013;57(7):3334-3339.
- Rodvold KA, Gotfried MH, Still JG, Clark K, Fernandes P. Comparison of plasma, epithelial lining fluid, and alveolar macrophage concentrations of solithromycin (CEM-101) in healthy adult subjects. *Antimicrob Agents Chemother*. 2012;56(10):5076-5081.
- Clewe O, Goutelle S, Conte JE, Simonsson USH. A pharmacometric pulmonary model predicting the extent and rate of distribution from plasma to epithelial lining fluid and alveolar cells—using rifampicin as an example. *Eur J Clin Pharmacol*. 2015;71(3):313-319.
- Lalande L, Bourguignon L, Bihari S, et al. Population modeling and simulation study of the pharmacokinetics and antituberculosis pharmacodynamics of isoniazid in lungs. *Antimicrob Agents Chemother*. 2015;59(9):5181-5189.
- Clewe O, Karlsson MO, Simonsson USH. Evaluation of optimized bronchoalveolar lavage sampling designs for characterization of pulmonary drug distribution. *J Pharmacokinet Pharmacodyn*. 2015;42(6):699-708.
- Derendorf H, Hochhaus G, Meibohm B, Möllmann H, Barth J. Pharmacokinetics and pharmacodynamics of inhaled corticosteroids. *J Allergy Clin Immunol*. 1998;101(4 Pt 2):S440-S446.
- Padden J, Skoner D, Hochhaus G. Pharmacokinetics and pharmacodynamics of inhaled glucocorticoids. *J Asthma*. 2008;45(Suppl 1):13-24.
- Hochhaus G. Pharmacokinetic and pharmacodynamic properties important for inhaled corticosteroids. *Ann Allergy Asthma Immunol*. 2007;98(2):S7-S15.